Hindawi
Journal of Advanced Transportation
Volume 2019, Article ID 6032305, 11 pages
https://doi.org/10.1155/2019/6032305

Research Article

An Airfield Soil Pavement Design Method Based on Rut Depth and Cumulative Fatigue

Duoyao Zhang, Liangcai Cai, and Shaohui Zhou

Engineering Institute, Air Force Engineering University, Xi'an, 710038, China

Correspondence should be addressed to Duoyao Zhang; zhangduoyao1990@yeah.net

Received 10 October 2018; Accepted 6 January 2019; Published 23 January 2019

Academic Editor: Jaeyoung Lee

The structure and damage modes of soil pavement, as well as existing problems in current design methods, were comprehensively analyzed, and a new design method for airfield soil pavement was proposed. The proposed method avoids the use of the "designed aircraft" concept and instead adopts the cumulative fatigue theory widely used in permanent airfield design at present. Moreover, in view of the lack of aircraft wheel trajectory distribution data, an approximate method for calculating the wheel trajectory distribution considering the side slip distance of the aircraft was proposed and the equivalent width of the wheel tread was calculated by introducing the modulus ratio. Finally, the pass-to-coverage ratio was obtained. According to the characteristics and damage modes of airfield soil pavement, rut depth was determined to be the unique factor affecting soil pavement damage, and resilient modulus was used as the control variable to improve the adverse impact of the empirical method. Furthermore, according to the rut prediction formula for airfield soil pavement put forward by the US Army Engineer Research and Development Center, a fatigue equation based on the resilient modulus was proposed to calculate the allowable number of repetitions. To verify the reliability of the design method, a test section was constructed at a test center in Jining, China, and the theoretical maximum allowable repetitions on the soil runway were calculated by the currently used California bearing ratio test, the β-fatigue equation, and the proposed method. Aircraft traffic tests were carried out on the test section. Finally, the theoretical and test results were compared and the values calculated via the proposed method were found to be consistent with experimental values, thereby validating the reliability of the method.

1. Introduction

The soil runway is a special type of runway that can be constructed quickly and is both flexible and easy to conceal and camouflage. With increasingly complex requirements of modern high-tech warfare logistics supply, strategic airdrop support capabilities, and combat and special missions, it has become the primary task of soil runways to ensure the effective take-off and landing of large transport planes. This requires complicated high load-bearing landing structures, thereby presenting new requirements for soil pavement design.

As early as the 1940s, relevant agencies represented by the US Army Engineer Waterways Experiment Station (WES), a subordinate unit of the US Army Corps of Engineers (COE) began to conduct experimental research on simple airfields. Based on the obtain series of results, specific standards for airfield design, construction, and restoration were defined [1]. In 1973, the US Air Force Flight Dynamics Laboratory completed a series of full-scale experiments on the "turning and high-speed linear rolling of aircraft on soil" using the tire-soil interaction straight test track at the University of Dayton in the US and studied the mechanism of interaction between the aircraft and soil pavement during taxi movement [2, 3]. Ladd and Ulery studied buoyancy characteristics during aircraft operation on a soil runway and plotted a nomograph to determine the strength of soil pavement according to the inflated tire pressure, equivalent single-wheel load, and number of coverages to failure [4]. Ladd and Barber introduced a design method to determine the optimal thickness of an unpaved soil runway for a C-5A Galaxy heavy-cargo transport aircraft [5]. Furthermore, Robert conducted traffic testing for the C-5A on a soil runway, evaluated the traffic performance and runway thickness, and finally obtained a standard equation for designing the soil runway thickness [6].

Development of pavement structure design was previously summarized by Ahlvin, who also reviewed the empirical formula for thickness of flexible pavement throughout different eras of the US military [7]. Grogan studied the requirements of gravel pavement suitable for supporting the operation of C-17 transport aircraft, and a full-scale test section was constructed. Currently, the US Army's unpaved runway structure standards, based on the 2- to 4-wheel main landing gear, are suitable for operating the C-17 aircraft [8]. These research results were used to develop the current soil pavement design method, namely, the California bearing ratio (CBR) design method for flexible pavement runways of permanent airfields. According to aircraft specifications and known soil strengths, the CBR curve can be used to design each structural layer and thickness of the support [9, 10]. However, several problems are associated with the application of this method to soil pavement design. For instance, during the "Allied Force" operation in 1999, the US military constructed a soil runway in the Kukes area, 50 miles north of Tiran Island. Although the soil runway was designed for the C-130 aircraft, it had to be shut down for maintenance after every 6–8 take-offs and landings. During the "Enduring Freedom" operation in 2001, the US military constructed a soil runway in Ruiroi, 80 miles southwest of Lakkan Daha, to ensure the transport of oversized equipment by the C-17 strategic transport. However, the runway required considerable reparations after every eight flights on an average. In both cases, the actual performance of soil runway did not meet the design specifications [8]. To reduce errors caused by empirical method, the American Air Force Civil Engineer Center proposed the β-fatigue equation, which partially solves the limitations of the pure CBR empirical method by introducing a semimechanical parameter β, while retaining the empirical CBR indicators in the formula [11].

Under the current backdrop, this study analyzes the structure and damage modes of soil pavement and the limitations of existing design methods. According to cumulative fatigue theory, a new design method for soil pavement was proposed, which adopted the rut depth as the only criterion to evaluate the damage of soil pavement and used the resilient modulus as the control variable. Reliability of the proposed design method was verified by onsite testing, with the objective of improving soil pavement design so that it is more suitable for real-world situations and can better meet the requirements of various types of aircraft, in particular, large heavy aircrafts.

2. Analysis of Soil Pavement Characteristics and Shortcomings of Current Design Methods

2.1. Structure of Soil Pavement and Damage Modes. Development of emergency airfields requires fast construction; however, these airfields usually have short usage periods, several weeks to years. Therefore, repetitive loading is less important in the design of temporary airfield pavements compared to those of permanent airfields. Moreover, the long-term effects on the natural environment can be ignored. Durability is not essential; therefore, as much as possible, the design of soil pavement structures should allow easy material selection and construction and the structural layer should be as thin as possible. Furthermore, if possible, locally available materials should be selected as the main components to reduce bulk material transportation requirements. Therefore, the most ideal runway is simple and can be developed using a simple construction onsite method, while meeting the requirements for a predefined number of aircraft take-offs and landings. The commonly used soil pavement structure consists of the reinforced base layer and pressed subgrade soil. If the base layer does not meet requirements, it can be paved or an additional layers can be added, which can take several forms such as an additional base layer, functional material, or assembled road panels, as shown in Figure 1.

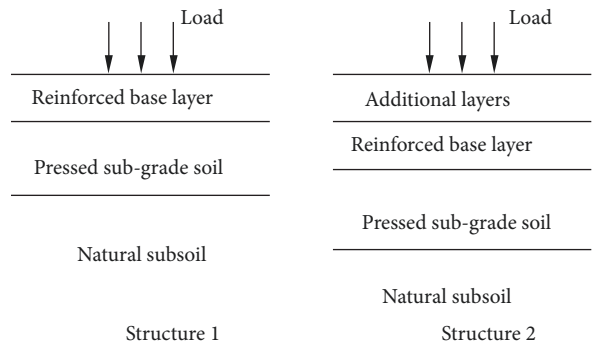

Figure 1: Illustrations of typical structures of soil pavement runways.

According to the operational characteristics of the soil runway, as well as observations and statistical data on damage conditions of airfield pavements, three main damage modes of soil pavement that occur under the combined action of the aircraft load and natural conditions can be defined: (1) fatigue cracks, temperature-shrinking cracks, and dry-shrinking cracks on the semirigid reinforced soil-pavement; (2) under the fatigue loading, permanent deformation on the surface layer and base layer leading to deformation damage caused by rutting; and (3) shear damage on the runway surface, wear of the surface layer, and pits and depressions caused by loose dust. The process of crack development in soil is similar to the generation of reflective cracks in pavement. Under high stresses, cracks gradually expand upward from the bottom of the layer. The process can be divided into three stages: "before fatigue cracking", "during fatigue cracking", and "after fatigue cracking". Owing to the short service life of soil pavement used for emergency airfields, cracks generated on the soil pavement under the aircraft load, in general, only reach the stage "before fatigue cracking". It still requires a certain period of development and evolution to reach the stage where the complete deterioration of pavement leads to fracture, so that the runway will not meet aircraft traffic requirements. At the same time, research indicates that even if cracks exist in the median and last stages, the soil pavement structure can maintain the state of "serving with cracks" [12]. Furthermore, functional damage to the soil pavement can be repaired. Comparative analysis indicates that rut deformation is the most common and significantly important damage mode. The surface layer is thin with low strength; therefore,

Figure 2: Formation of rutting on the soil pavement during aircraft take-off and landing.

the aircraft load can generate large rutting on the surface layer at the beginning stages of base layer fatigue cracking. This phenomenon is more pronounced during take-off and landing of aircraft with large loads and high tire pressure (Figure 2). Large aircraft can successfully take off and land on a soil runway under two conditions. First, the aircraft must have a large number of main wheels, which reduces tire pressure and distributes the forces acting on the surface more uniformly. Second, the aircraft landing and taking off from soil runways must be specially modified, for example, a special thrust reversal can shorten the landing distance and reduce the rutting effect by discharging airflow from the engine to the aircraft body at a certain angle.

2.2. Analysis of Current Design Method. The main limitations of the current soil pavement design methods are reflected in two aspects. More important aspect is that the CBR method has large disadvantages when applied to the design for soil pavement:

(1) The CBR design method was developed from design practices used for road pavement and improved upon by the multi wheel heavy gear load full-scale test to the airfield pavement design method which can be applied to the aircraft traffic load and wheel configuration. The results obtained by the empirical method are related to the observed pavement as well as the materials, environment, and loading conditions of the full-scale test. If the conditions for the specially designed pavement are similar to the conditions for which the method was originally developed, a satisfactory design can be obtained. However, due to differences in environmental conditions, rapid development of traffic loads, and emergence of new materials, it is necessary to continuously extend the empirical relationship. Thus, applicability of the CBR method is limited because it was established for the design of permanent airfields [13, 14]. Although strict standard controls, a sufficient construction period, and suitable remedies can limit the design error to be within an acceptable range for permanent airfields, the situations for the use of soil pavement are completely different. The material used in the construction of soil pavement is often obtained locally, the construction period is shorter, and the materials and environments can differ significantly. As result, application of CBR design methods to soil pavement can produce huge errors that cannot be ignored.

(2) The CBR value is only an empirical index and not a direct measurement of the load bearing capacity of a material. Therefore, it has little relationship with the elastic deformation of the subgrade soil of airfield pavement. However, the actual pavement structure design requires the CBR value to work under the elastic stress. Under these working conditions, the shear strength of subgrade soil characterized by the CBR value is not important in the pavement design, but resilient properties (resilient modulus) of subgrade soil and plastic deformation under repeated loading [15].

(3) The CBR design method cannot accurately characterize the damage mode of soil pavement. The most important point is that the CBR design method considers rutting damage on the pavement surface to be the result of excessive stress on the soil base layer and the in-layer deformation generated within each pavement layer can be ignored. In fact, due to the low strength of the surface layer of soil pavement, rutting on the pavement surface is attributed more so to the in-layer deformation within the pavement structure. Moreover, the fatigue cracking and low-temperature cracking of the surface layer and other damage modes of the pavement structure, which can be the main damage modes of the soil pavement, cannot be characterized using CBR.

(4) With the emergence of a new generation of large aircraft, the configuration of the landing gear has become increasingly complicated, indicating that the weight of aircraft, the number of tires, the shape of the wheel treads, and the tire pressure have changed greatly. As a result, the original CBR curve has not been able to meet the requirements of the new generation of large aircraft. Based on the existing method, the US Federal Aviation Administration (FAA) has shown that the results of the CBR method are too conservative and the method performs poorly in most engineering applications [16].

Current design of soil pavement still adopts the concept of "aircraft in design," even though it has been confirmed that the theory leads to large errors in the design of permanent airfields [17, 18]. Moreover, errors are inevitably generated when converting the traffic volume of other aircraft models into the traffic volume of aircraft during the design process. Therefore, the wheel trajectory distribution of different aircraft models on the runway is not the same, but this is not reflected in traffic volume conversions.

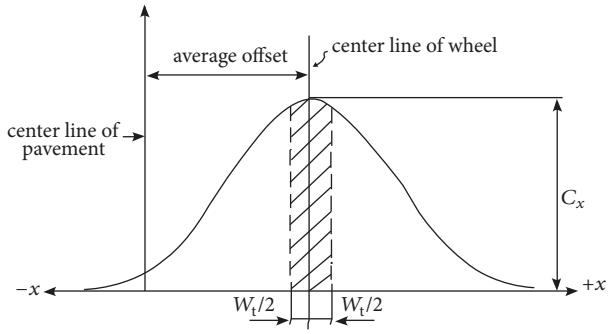

Figure 3: Schematic representation of pass-to-coverage ratio calculation.

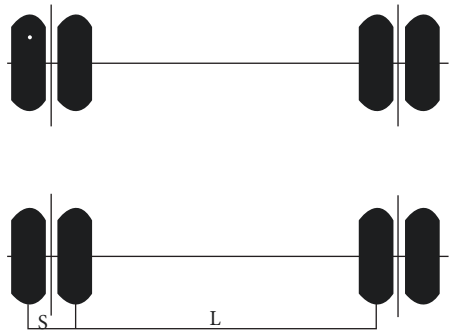

Figure 4: Schematic illustration of the structure of A-type transport aircraft main wheels.

3. Calculation of Number of Repetitions on Actual Pavement

3.1. Pass-to-Coverage Ratio. The method proposed in this study calculates the actual repetitions for soil pavement by a traffic volume prediction model based on cumulative damage, also known as the number of coverages in traffic. The effect of the aircraft on the pavement structure is transmitted through the landing gear wheels. When the adopted aircraft passes the pavement and generates a maximum stress (or strain) on a certain point, this is considered one "coverage." The pass-to-coverage ratio is the ratio of the total number of passes on the runway cross section to the number of coverages at a certain point [19]. According to a large number of investigations and analyses, the trajectory distribution of an aircraft's wheel on a runway and taxiway can be approximated as normal distributions. For the design of airfield pavement, the actual factor influencing the structural thickness is the number of coverages of the point subjected to the maximum repeated action of the aircraft wheels, that is, the midpoint of the trajectory distribution, as shown in Figure 3. Assuming the effective width of the tire to be W_t, for the center point the single wheel whose center line is within $-W_t/2$–$W_t/2$ can act on the center point and coverages. Therefore, the pass-to-coverage ratio at this time can be calculated [20]:

$$\frac{P}{C} = \frac{1}{C_x W_t} \tag{1}$$

where C_x is the probability density at the center of the normal distribution curve of the wheel trajectory and W_t represents the effective width of the tire.

3.2. Superimposing Wheel Trajectory Distributions. In contrast to the wheel trajectory distribution of aircraft on permanent airfields, which is supported by a huge amount of data, relatively little statistical data exist on the wheel trajectory distribution of aircraft on soil runways. Only the full-scale test of the ERDC can provide the simple wheel trajectory distribution as the running conditions of the C-17 aircraft must be simulated on actual soil pavement. Therefore, in the wheel trajectory distribution 2, the standard deviation σ and mean value μ of the wheel normal distribution curve can only be estimated by calculations. According to the test for the wheel trajectory curve of a permanent airfield, the center line of the runway is considered the baseline when the aircraft takes off or lands on the runway. Therefore, the distribution center of the overall center line of the aircraft should be the center line of the runway.

For a single-wheel aircraft, the mean value μ of the main wheel trajectory distribution on both sides is set to be $\pm L/2$, where L is the track between left and right main wheels. The probability density at the center of the normal distribution curve of the right wheel tread can be obtained by using (2). Furthermore, the formula for calculating the standard deviation of the wheel trajectory distribution on the soil runway is given in literature report [20] and can be expressed as (3) as follows:

$$C_x = f(x)\big|_{x=L/2} = \frac{1}{\sigma\sqrt{2\pi}} e^{-(1/2)((x-L/2)/\sigma)^2}\Big|_{x=L/2} \tag{2}$$

$$\sigma = \frac{W_w/2}{1.15} \tag{3}$$

where L represents the track between the left and right main wheels, σ represents the standard deviation of the normal distribution curve of the wheel tracks, and W_w represents the sliding width of the wheels when the aircraft is taxiing. The actual number of coverages at this point can be obtained by dividing the actual number of passes by the pass-to-coverage ratio.

For large aircraft, the main landing gear is more complicated in general, with single-axle multiple wheels and even multiple-axle wheels. When a large aircraft is taxiing on the runway, each main wheel can pass any point on the runway and generates stress on that point. Therefore, to calculate the pass-to-coverage ratio of large aircraft, it is necessary to superimpose the tracks of all the main wheels. For multiwheel aircraft, the average value of the trajectory distribution of the left and right inner main wheels is $\pm L/2$, where L represents the track between left and right inner main wheels of the aircraft. The right main wheel of a military transport (herein referred to as the A-type transport aircraft) is considered as an example and the landing gear configuration is presented in Figure 4. Clearly, the main landing gear belongs to the typical two-axle two-wheel type. First, the trajectory of the main wheel of the right rear axle is superimposed, and the

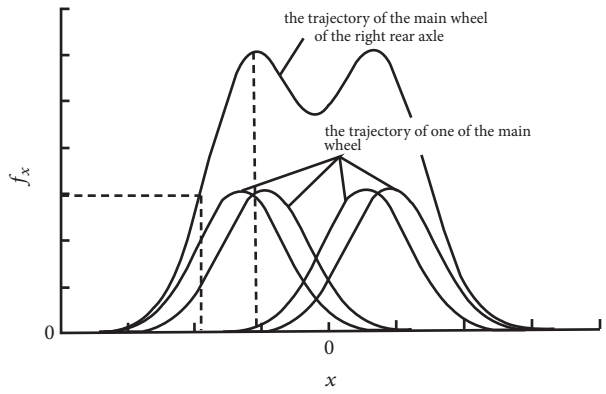

Figure 5: Wheel trajectory distribution of main wheels of rear axle (after superposition).

probability density is obtained as (4). Next, the trajectory of the main wheel of the left rear axle is superimposed; and finally, the trajectories of the left and right rear axles are superimposed to obtain the trajectory distribution of the rear axle main wheel, as shown in Figure 5.

$$f(x) = \frac{1}{\sigma\sqrt{2\pi}}\left[e^{-(1/2)((x-L/2)/\sigma)^2} + e^{-(1/2)((x-L/2-s)/\sigma)^2}\right] \quad (4)$$

where S represents the track between the main wheels on the same side and L represents the track between the inner main wheels on left and right sides.

According to literature [19], when each axle of the multi-axle landing gear sequentially passes a point on the semirigid or flexible pavement, maximum stress is generated as each axle passes, that is, one coverage occurs. The front and rear main wheels on the right side of the A-type transport aircraft are exactly the same in number and configuration; therefore, the wheel trajectory distribution sets are also consistent. As the main wheel passes the point, it forms two coverages. Therefore, by multiplying (4) and (2), we obtain the wheel trajectory distribution after superimposing the two main wheels on the right side, expressed as (5) as follows:

$$f(x) = \frac{2}{\sigma\sqrt{2\pi}}\left[e^{-(1/2)((x-L/2)/\sigma)^2} + e^{-(1/2)((x-L/2-s)/\sigma)^2}\right] \quad (5)$$

Figure 5 illustrates that the aircraft tires have the most repeated actions at a position close to the center of the two main wheel gaps. By substituting (5) into (2), the probability density formula at the trajectory center of the right main wheel is obtained, which is given by (6) as follows:

$$C_{xc} = f(x)\big|_{x=L/2+s/2} = \frac{2}{\sigma\sqrt{2\pi}}\left[e^{-(1/2)((x-L/2)/\sigma)^2} + e^{-(1/2)((x-L/2-s)/\sigma)^2}\right]\Big|_{x=L/2+s/2} \quad (6)$$

3.3. Effective Tire Width. Under the load of the aircraft wheel, bending stress is generated at the bottom of pavement. Calculation of cumulative damage not only includes the damage at the position of the maximum stress point, but also damage within the area surrounding the maximum stress point as this area experiences stress close to the maximum stress. As the wheel load passes the area once, every point within the area produces approximately the same fatigue damage. In turn, to calculate the number of coverages at a particular point, the traffic volume within a stress area around the point causes one-time fatigue damage. The lateral distance of the stress area generated by the wheel is defined as the effective tire width, which refers to the length when the wheel mark width is projected onto the soil base at a certain diffusion angle. For flexible asphalt, a diffusion ratio of 1:2 was selected. For cement–concrete pavement, the diffusion angle of the load was taken to be zero [21]. The strength of the semirigid stable soil pavement was between that of flexible asphalt and cement–concrete pavement. Therefore, the conversion method for the equivalent wheel tread width of a permanent airfield could not be applied. In view of the situation, the ratio of the strength of the surface layer to the strength of the soil base (modulus ratio) can be taken as the standard, and the effective tire width of the large aircraft on the soil pavement can be calculated as follows [22]:

$$W_t = 2hk + W_0 \quad (7)$$

$$\lambda = \frac{E_2/\left(1-\mu_1^2\right)}{E_1/\left(1-\mu_0^2\right)} \quad (8)$$

$$k = \tan\theta = 0.133 + 0.095\lambda^{0.208} \quad (9)$$

where h is the thickness of reinforced base layer; E_1 and E_2 are the resilient moduli of the compact soil base and reinforced base layer, respectively; μ_1 and μ_2 represent the Poisson's ratio of the soil base and reinforced base layer, respectively; λ is the generalized modulus ratio; θ represents the load diffusion angle; k denotes the proportion of load diffused, and W_0 is the width of wheel tread.

3.4. Calculation of Slip Width. According to literature [23], the slip width is not actually a fixed value but changes with the aircraft taxiing distance on the runway. The maximum slip width consists of the distance from the initial take-off/landing positions to the runway center line and the taxiing distance on the runway. Factors affecting the taxiing distance include the sideslip angle on landing, wind speed, and sideslip coefficient. The sideslip coefficient is related to the frictional resistance and the longitudinal and transverse slopes of the pavement. The calculation method for slip width based on reliability was also given. According to the method reported in literature [12], the sideslip distance of an A-type transport on a soil runway under different friction coefficients could be calculated, as presented in Table 1.

4. Allowable Number of Coverages

According to the analysis in Section 3, rut damage is the most important damage mode of soil pavement. Therefore, rut deformation was selected as the only standard for controlling damage to the soil pavement structure. Based on a large

Table 1: Sideslip distances of A-type transport under different friction coefficients.

Friction Coefficients	0.55	0.60	0.65	0.70	0.75	0.80	0.85	0.9
Sideslip distances (m)	5.34	5.13	4.96	4.68	4.54	4.40	4.28	4.18

number of full-scale tests, the ERDC has provided a predictive formula for rutting on the soil pavement of temporary airfields [11]:

$$R_d^0 = 0.1741 \frac{p^{0.4707} q^{0.5695} N^{0.2476}}{(\log h)^{2.002} C_1^{0.2848} C_2^{0.9335}} \tag{10}$$

$$R_d = \phi R_d^0 \tag{11}$$

where h is the thickness of reinforced base layer, in; N is the number of passes; p represents the equivalent load of single wheel, kips; q represents the tire pressure, psi; R_d^0 represents rutting of soil pavement for calculation, in; R_d is the rutting on the soil pavement after correction, in; C_1 is the strength of the CBR value for the compacted soil base; C_2 is the strength of the CBR value for the reinforced base layer; and ϕ is the correction factor. The correction factor is related to the material properties of the surface layer. If there is no surface layer, ϕ is 1.

To improve the empirical method, the formula for conversion between the CBR and resilient modulus can be represented [20] as Eq. (12). Substituting (11) and (12) into (10), a relationship between the number of repetitions on the soil runway and the rut depth can be obtained. For WES [9], the rut depth on the soil runway should not exceed 76 mm (3 in); therefore, an equation for the allowable number of repetitions for soil pavement can be defined as (13)

$$E_0\,(psi) = 1800 CBR^{0.7} \tag{12}$$

$$N = \left(\frac{(\log h)^{2.002} E_1^{0.4069} E_2^{1.3336}}{26872.11 \cdot p^{0.4707} q^{0.5695}} \right)^{4.04} \tag{13}$$

5. Soil Pavement Design Method Based on Cumulative Fatigue Principle

5.1. Design Principle. The soil pavement design method adopts the FAA ordinary concrete pavement design method based on cumulative damage. According to the Miner principle, the extent of fatigue damage due to different aircraft is linearly accumulated and a cumulative fatigue damage factor (CDF) can be obtained. Based on whether the CDF is close to 1, we can determine if the pavement has reached fatigue destruction [24, 25]:

$$CDF = \sum_{i=1}^{m} CDF_i = \sum_{i=1}^{m} \frac{n_i}{N_i} \tag{14}$$

$$n_i = \frac{N_i^t}{P/C} \tag{15}$$

where N_i^t represents the number of passes of the I-type aircraft and n_i represents the number of actual coverages made by the I-type aircraft.

5.2. Design Procedure. In soil pavement design, the expected usage time of the soil pavement should first be determined. Then, according to the characteristics defined to guarantee the task and use requirements of the soil pavement emergency airfield, the load parameters of every aircraft model using the runway are acquired. Moreover, the increase in traffic volume owing to take-off and landing modes, as well as the sortie and the follow-up tasks, is predicted. Based on the surrounding environment, soil quality, and material conditions of the proposed location, the pavement combination and form are preliminary fitted to determine the thickness and parameters of each structural layer and of the soil-based materials. Subsequently, the predicted traffic volume and pavement structure are used to calculate the pass-to-coverage ratio of each aircraft as well as the expected coverages during the design period. Furthermore, based on the fitted pavement combination, the maximum compressive stress under each aircraft load can be calculated and the soil pavement fatigue equation can be adopted to calculate the allowable number of actions of each aircraft. Finally the cumulative damage factor for each aircraft is calculated and linearly superimposed and compared with 1 to regulate the pavement thickness. A flowchart of the design process is presented in Figure 6.

6. Validation of Design Method

In this study, the reliability of the new design method was validated by onsite traffic testing. The test section was constructed at an Air Force test center in Jining, China. First, theoretical calculations were carried out. A theoretical soil runway with the parameters identical to those of the test section was fitted to guarantee take-off and landing of A-type transport aircraft. Some of the fitted parameters are listed in Table 2. Using the relevant test section parameters and the test aircraft model, the theoretical maximum allowable repeated actions on the soil runway were calculated employing the currently used CBR method, the fatigue equation, and the proposed method. Then, a traffic test was carried out on the test section to obtain the theoretical maximum allowable repeated actions for the A-type transport aircraft on the soil pavement. Finally, the theoretical calculation results and experimental results were compared.

6.1. Setup of Test Section. The soil pavement of the test section was previously described in literature report [26] and was 50 m in length and 7.5 m in width, as shown in Figure 7. From bottom to top, the test section was comprised of a compacted soil base and reinforced base layer, both with a thickness of 300 mm, as shown in Figure 8. The reinforced subgrade soil was composed of 5% composite Portland cement (PO32.5, Zhangshan Cement Plant, Shandong Province), 4% lime (Jiaocheng Guihe Lime Plant of Shandong Province), 0.015% stabilizer (TG-2 soil stabilizer, Beijing Yilu Tetong New Materials Co., Ltd.), and Jining soil. The main components and performance parameters of the soil base layer are listed in Table 3.

According to the "Field Test Methods of Subgrade and Pavement for Highway Engineering" (JTG E60-2008) [27], the CBR value, resilient modulus, Poisson's ratio, and friction

Table 2: Partial parameters of A-type transport aircraft.

Type	Maximum mass during take-off (kN)	Load distribution coefficient of main landing gear	Single-wheel load of main landing gear (kN)	Tire pressure (MPa)	Area of wheel tread (m^2)	Wheel tread width (m)	Distance between wheel on the same side (S/m)	Width of inner track between left and right main wheel (L/m)
A-type transport aircraft	620	0.95	79	0.78	0.111	0.2764	0.490	4.43

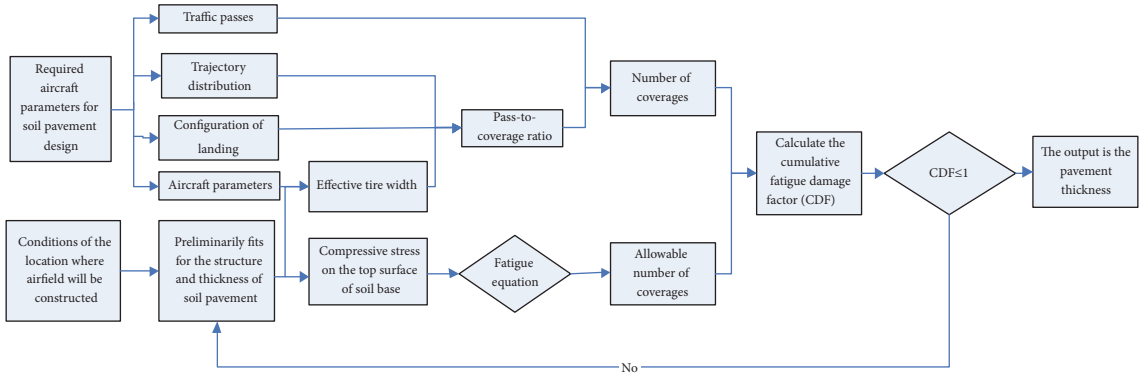

Figure 6: Flowchart of pavement design process.

Figure 7: Onsite conditions of test section.

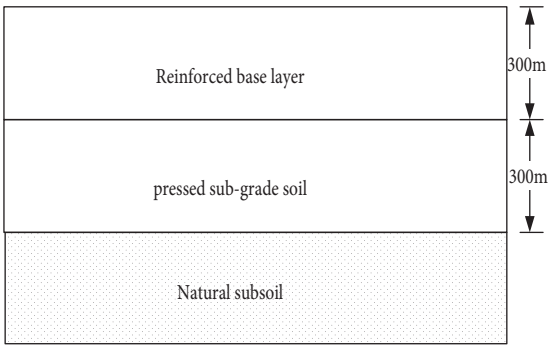

Figure 8: Schematic illustration of test section.

coefficient of the test section were determined. The average values of five points were used for each parameter. If the difference between the measured value and the mean value exceeded 15%, the point was remeasured and the new data were included to the list of existing data for recalculation. The final integrated resilient modulus of the subgrade and soil base of the test section was 118 MPa and 54 MPa, respectively, and the CBR values were 24 and 8, and the Poisson's ratio was 0.25.

6.2. Theoretical Calculations

6.2.1. CBR Method. The *Planning and Design of Roads, Airfields, and Heliports in the Theater of Operations–Airfield and Heliport Design* (FM 5-430-00-2, US Army) [9] provide a complete set of CBR design methods for soil pavement (using C-17 and C-130 as aircraft in the design). Figure 9 shows the relationship between the allowable passes and the CBR of the soil base. The reinforced base layer acts as a cushion over the soil base. No matter which type of cushion the base layer belongs to, when the CBR value of the soil base is 9, the soil runway allows the C-17 to pass at least 900 times. Noteworthy, one pass includes one take-off and one landing. The load during take-off and landing on the soil runway is 50% of the maximum load; therefore, the maximum number of passes under the maximum load is 900 times as well. The equation for converting the passes of other aircraft and aircraft in design is given by literature report [28].

$$\log N_{di} = \left(\frac{P_i}{P_s}\right)^{0.5} \log \delta N_i \tag{16}$$

where N_{dt} is the number of passes after the conversion; N_i represents the number of passes of the aircraft to be

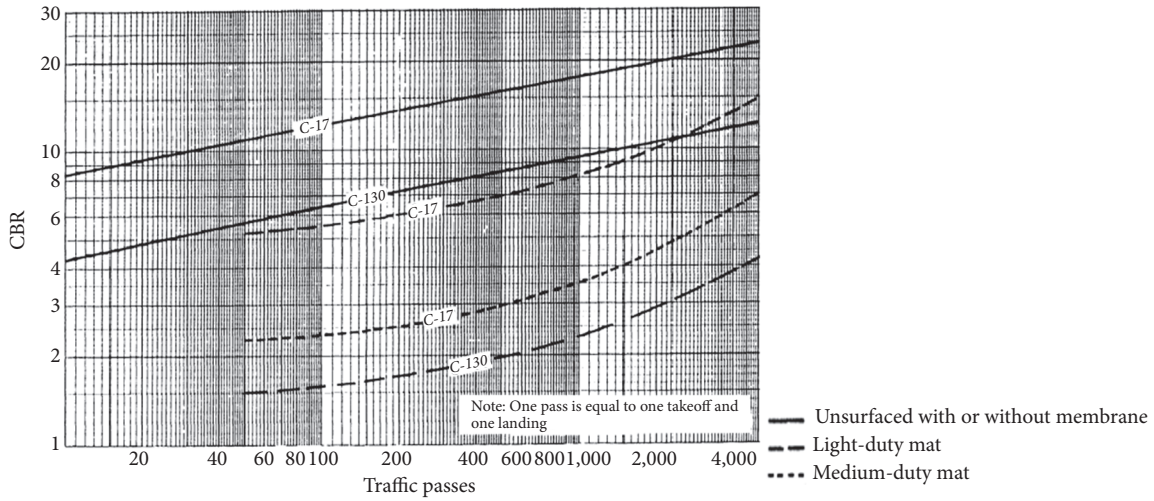

Figure 9: Relationship between allowable traffic passes and CBR of soil base (aircraft in design).

Table 3: Main components and properties of soil base.

Name	Property Parameters				
Jining soil	Liquid limit (%)	Plasticity limit (%)	Plasticity Index	Maximum Dry Density (g cm^{-3})	Standard name
	30.6	17.5	13.1	1.9	Low-liquid limit silt
Soil Stabilizer	Appearance characteristics	Concentrated solution	unit weight (25°C)	Solidification Point/°C	Content of anionic surfactant (mass %)
	Dark red	0.5–1.0	1.00 ± 0.01	<0	8.4
Lime	State of sample	Test standard	CaO and MgO contents (%)		Conclusion
			First-rate product	Measured value	
	Normal	JC/T 481-92	≥ 60	69	Mg-based slaked lime powder with MgO content of 13.18%

converted; P_s represents the load of one main wheel of the aircraft used in the design; P_i is the load of one main wheel load of the aircraft to be converted (one main wheel load of C-17 is 199.48 kN); and δ is the structure conversion factor of the landing gear. Herein the three-axle two-wheel landing gear was converted to the two-axle two-wheel landing gear; therefore, δ was set as 0.8. (The aircraft's weight did not change, while the number of main wheels supporting the most weight of aircraft increased from 12 for three-axle two-wheel configuration to 8 for two-axle two-wheel configuration. Thus the load on the former landing gear was around 0.7 times of that on the latter landing gear. With consideration of the variation in the distribution coefficient of main landing gear and safety factor, the value was increased to 0.8). The allowable passes for an A-type transport aircraft with maximum load was approximately 48700.

Noteworthy, the sum of all pass numbers for certain aircraft models was calculated. The number of repetitions for each point could be obtained if only the wheel trajectory distribution was calculated. According to the parameters listed in the test section and Table 3, the equivalent wheel tread width of the A-type aircraft was 0.429 m, as obtained from (7)–(9). The friction coefficient of the test section was 0.66. Table 1 summarizes that the slip width of the A-type transport aircraft on the soil pavement should be between 4.68 and 4.96 m. Herein, the slip width was considered as 4.7 m and the standard deviation of the wheel trajectory distribution of the A-type transport aircraft (the right main wheel) was 2.043. The relevant parameters were substituted into (1) and (6), and the probability of passing the point with the highest number of passes was 0.32. Furthermore, the allowable number of repetitions was calculated to be 15500.

6.2.2. β-Fatigue Equation. The β-fatigue equation can be expressed as follows:

$$\log \beta = \frac{a + b \cdot \log N}{1 + c \cdot \log N} = \frac{1.8451 + 0.1914 \cdot \log N}{1 + 0.3193 \cdot \log N} \quad (17)$$

$$\beta = \frac{145\pi \cdot \sigma}{C_R} \quad (18)$$

Table 4: Theoretical and test results.

method	CBR method	β-fatigue equation	proposed method	test results
the allowable number of repeated coverage.	15500	3384	1981	1600

Figure 10: Photograph of loading vehicle.

where N represents the allowable number of repeated coverages, σ is the compressive stress on the top surface of the soil base, MPa, and C_R is the CBR value representing the strength of the soil base.

Finite element analysis was used to determine the maximum compressive stress on the top surface of soil base under the action of an A-type transport aircraft, $\sigma = 0.269$ MPa. Moreover, the measured CBR was 8; therefore, the allowable number of repeated actions on the soil pavement was calculated to be 3384.

6.2.3. Proposed Method. The thickness of the reinforced layer was 300 mm, the resilient moduli of the base layer and soil base were 118 MPa (17110 Psi) and 54 MPa (7830 Psi), respectively. The equivalent single-wheel load of the A-type transport aircraft was 316 kN (71.8 kip), and the tire pressure was 0.78 MPa (113 Psi). Substituting the values in (13), the allowable number of repeated actions was calculated to be 1981.

6.3. Passing Test. A loading vehicle was used to simulate the traffic load of a certain type of military transport aircraft, as shown in Figure 10. The auxiliary wheel can be raised using a hydraulic device (relative to the loading wheel) to ensure that most of the load is applied through the loading wheel. The loading wheel represents one landing gear of the A-type transport aircraft. The landing gear has four main wheels with a maximum load of 320 kN and main tire pressure of 0.78 MPa. During the test, the tractor towed one side of the loading vehicle and loading was carried out in a forward–backward manner to ensure that all loads were repeatedly applied to a single wheel trajectory; that is, two coverages occurred during each loading. One unit was considered to be 100 loading times. Once 100 loadings were reached, the process was paused for 2 min and the value was read. Rutting was tested using a cross-sectional instrument. During testing, the rut depths of two lanes were read and the average value was taken as the rut depth of the section. Figure 11 shows the variation of rut depth with loading time. When the number of repetitions reaches 1600, the rut depth is 74 mm and destruction of the road surface is evident.

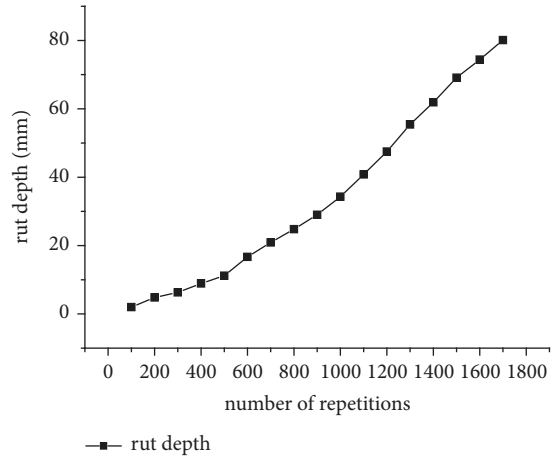

Figure 11: Variation of rut depth with increasing loading time.

Figures 12 and 13 show the surface and bottom of the base layer and the soil base after loading (after excavation). Clearly, except for some rut damage, the structural integrities of the base layer and the soil base are both well maintained and there is no obvious cracking. The area outside the rut on the base layer is also relatively flat and there is a large depression. When rut damage occurs, other types of damage have not yet formed, which again indicates that rutting is the main form of damage to soil runways.

6.4. Analysis of Test Results. By comparing the theoretical results with the test results for the maximum allowable number of repetitions (Table 4), the following conclusions can be drawn:

(1) The theoretical results calculated by the CBR method are much larger than the actual values, which is consistent with the performance of the soil runways constructed by the US military. The reasons are outlined in Section 2.2. The CBR method uses empirical parameters and is unable to

Figure 12: Surface condition of base layer.

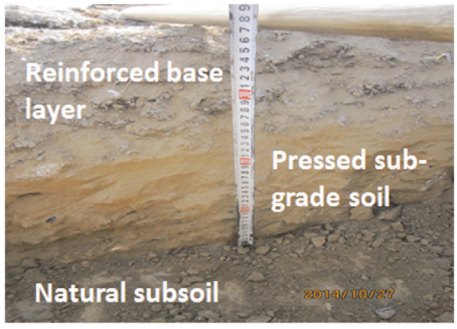

Figure 13: Conditions of bottom part of base layer and soil base after construction has begun.

characterize the most common damage mode of soil runways, which is rut damage. Furthermore, the traffic volume conversion between the aircraft required in the design magnifies the error; thus the method should be avoided in future soil runway design as much as possible.

(2) The β-fatigue equation is closer to reality than the original CBR method, indicating that it is correct to avoid using the purely empirical method; however, the β-fatigue method still results in large errors. The equation still uses the CBR values as the control. As a result, the self-imposed limitations of the CBR method cannot be completely eliminated. Moreover, the equation mainly represents shear damage to the base layer.

(3) Comparatively, the value obtained by the proposed method is the closest to the test results, indicating that the design of the soil runway of emergency airfield is feasible using rut depth as the controlled standard and the resilient modulus of the soil base as the controlled variable, verified by the results presented in Figures 12 and 13.

(4) Noteworthy, although the values obtained by the method proposed in this study are the closest to the test results, error still exists, almost 400 times. The analysis indicates that besides the test error, the fatigue equation used in this study is also employed to perform calculations using the CBR value as the control amount which is then converted into the resilient modulus of soil base via an equation. Therefore, a certain amount of error inevitably occurs during the conversion process and magnifies the overall error. On the other hand, the fatigue equation used in the study is also based on tests and some errors are associated with different environments. To reduce this error, it is necessary to perform several experiments in order to modify the fatigue equation, which will be the main direction of future research.

7. Conclusions

This study comprehensively analyzes the shortcomings of the existing design method and proposes a novel design method for the soil pavement of airports. The proposed method adopts the pavement fatigue theory based on pass-to-coverage ratio, adopts the rut depth as the criterion to evaluate the damage of soil pavement, and uses the resilient modulus as the controlled variable. Through on-site passing test, it can be found that the theoretical calculation results provided by the proposed method are closer to experimental results than other design methods, which validates the method's credibility.

Future research will aim to continuously modify the fatigue method based on a large number of experiments to improve its accuracy and extend the range of applications of the fatigue equation.

Data Availability

The [experimental data and parameter plane] data used to support the findings of this study are included within the figures and tables.

Conflicts of Interest

The authors declare no conflicts of interest regarding the publication of this paper.

Acknowledgments

This work was financially supported by the National Natural Science Foundation of China (ID: 51578540 and ID: 51608526).

References

[1] T. Tan, L. C. Cai, X. J. Liu et al., "Research on design method of soil expedient airfield runway," *Journal of Air Force Engineering University (Natural Science Edition)*, vol. 13, no. 6, pp. 11–14, 2012.

[2] *Landing Gear/Soil Interaction Development of Criteria for Aircraft Operation on Soil during Turning and High Speed Straight Roll*, University of Dayton, Dayton, Ohio, USA, 1974.

[3] *Landing Gear/Soil Interaction Development of Criteria for Aircraft Operation on Soil during Turning and Multipass Operation*, University of Dayton, Dayton, Ohio, USA, 1975.

[4] A. T. Pereira, "Procedures for development of CBR design curves," Flexible Pavements, 1977.

[5] C. C. Frank, *Performance Capabilities of the C-5 and C-17 Cargo Aircraft*, U.S. Army Engineer Waterways Experiment Station, Vicksburg, Mississippi, USA, 1984.

[6] E. W. Hansen, *Evaluating the C-17 Semi-Prepared Runway Capability an Off-Road Map*, Air force institute of technology graduate school of engineering and management, 2002.

[7] G. Ahlvin Richard, "Origin of Developments for Structural Design of Pavements," Tech. Rep. GL-91-26, USAE Waterways Experiment Station, Vicksburg, MS, USA, 1991.

[8] *Evaluation the C-17 Semi-Prepared Runway Capability-An off-Road Map*, Air Force Institute of Technology, 2002.

[9] *Report Simple Track Research and Application at Home and Abroad*, Air Force Engineering University, 2015.

[10] *Planning and Design of Roads, Airfields, and Heliports in the Theater of Operations-Road Design Volume I*, ArmyDepartment of the Air Force, Washington, DC, USA, 1994.

[11] S. Zhou, *H Luminum Honeycomb Truss Panel Pavement Structure Design Method of Research*, Air Force Engineering University, 2016.

[12] J. Z. Liu, *Research on Emergency Soil Airfield Pavement and Material*, Air Force Engineering University, 2007.

[13] K. Gopalakrishnan, *Performance Analysis of Airport Flexible Pavements Subjected to New Generation Aircraft*, University of Illinois at Urbana-Champaign, 2004.

[14] B. Rodway, "The impact of new-generation large aircraft on the structural design of flexible pavements," *Scientific Research on Aging*, vol. 4, no. 6, article no. 4052, 1995.

[15] F. Brown S, "Achievements and challenges in asphaltengineering," in *Proceedings of the International Conference on Asphalt Pavements*, pp. 26–36, 1997.

[16] W. Liu, *Study on Design Indexes and Methods for Asphalt Airport Pavement*, Tongji University, 2008.

[17] A. Wu H, L. Cai C, Q. Gu K et al., "Airport concrete pavement design for large aircraft in future," *Journal of Beijing University of Aeronautics and Astronautics*, vol. 37, no. 9, pp. 1169–1175, 2011.

[18] Q. S. Li, H. D. Zhao, and J. M. Ling, "Method of airport concrete pavement design for large military transport aircrafts," *China Civil Engineering Journal*, vol. 44, no. 1, pp. 121–126, 2011.

[19] A. H. Wu, L. C. Cai, Q. K. Gu et al., "Analysis of pavement traffic volume using pass-to-coverage ratio," *Journal of Traffic and Transportation Engineering*, vol. 10, no. 6, pp. 82–88, 2010.

[20] AC 150/5335-5A, "Standardized method of reporting airport pavement strength-PCN," 2014.

[21] D. Zhao H, *New Generation Large Aircraft Oriented Load Analysis Method and Parameters for Asphalt Pavement Design*, Tongji University, 2007.

[22] H. D. Zhao, J. M. Ling, and Z. K. Yao, "Simplified methods for calculating aircraft load repetition," *Journal of Tongji Univeristy(Natural Science)*, vol. 39, no. 5, pp. 693–698, 2011.

[23] S. Lu, *Research on Military Airfield Design Based on Reliability Theory*, Air force engineering university, 2007.

[24] AC 150/5320-6E, "Airport Pavement Design and Evaluation," 2009.

[25] D. R. Brill, *Calibration of FAARFIELD Rigid Pavement Design Procedure (DOT/FAA/AR-09/57)*, Federal Aviation Administration (FAA), 2010.

[26] J. Z. Liu, X. Z. Weng, J. Zhang et al., "Model experiment of fatigue deformation characteristic of emergency soil airfield pavement," *Journal of Southwest Jiaotong University*, vol. 49, no. 3, pp. 412–418, 2014.

[27] JTG E60-2008, "Field test methods of subgrade and pavement for highway engineering," 2008.

[28] GJB 1278A -2009, "Specifications for design of cement concrete pavement for military airport," 2009.